# High-resolutional Calorimetric Study on Solid Solutions $SnCl_2(H_2O)_x(D_2O)_{2-x}$

Masami TATSUMI,† Takasuke MATSUO, Hiroshi SUGA, and Syûzô SEKI*

*Department of Chemistry, Faculty of Science, Osaka University, Toyonaka, Osaka* 560

(Received September 4, 1978)

Heat capacities of the system of solid solutions $SnCl_2(H_2O)_x(D_2O)_{2-x}$ ($x$=2.00, 1.97, 1.75, 0.96, 0.50, 0.25, and 0.03) were measured by an adiabatic calorimeter capable of determinations of heat capacity with the temperature step of 5—10 mK. The heat capacity peak due to order-disorder change of hydrogens becomes broader and its transition temperature rises as the deuteron concentration is increased. A small first-order component was found in the crystals of $x$=2.00, 1.97, and 1.75. Measurements were repeated for aged crystals of $x$=0.96, 0.50, and 0.03. Nature of the phase transition has been discussed in analogy with the liquid-vapor critical point. From the heat capacity data around the glass transition it is concluded that the motion of the hydrogen atoms is strongly correlated with each other over a range whose size is large enough that fluctuation of the local isotopic composition from the average is negligible.

The phase transition in tin(II) chloride dihydrate $SnCl_2 \cdot 2H_2O$ (abbreviated as TCD) was discovered by Kiriyama *et al.*[1] The complete crystal structure was determined by them by using the X-ray[2] and the neutron diffraction[3] techniques. The crystal consists of layers of tin(II) chloride molecule alternating with layers of water molecules. There are two types of water molecules in the layers. One of them, designated as $H_2O$ (1), is coordinated to the tin(II) ion and the other, $H_2O$ (2), is a water of crystallization. Each type of water molecules is hydrogen-bonded to three others of different type in the same layer parallel to the (100) plane. In the hydrogen bonding network, there are seven kinds of positions which deuterons can occupy and the three types of hydrogen bond with different bond length.[4-7] The O(2)···O(1′) hydrogen bond differs from the other two in that its bond length increases anomalously below $T_c$, in contrast to the other two which contract as the temperature is lowered.

An unusual property of the phase transition in TCD is that there occurs no change of symmetry of the crystal at the transition, including that pertaining to the hydrogen atom. The space group is $P2_1/c$ both below and above the transition. No symmetry elements are lost or gained on passing through the transition. It is generally assumed that a phase transition of any substance is accompanied by a change of symmetry of the substance. The symmetry in question may be that of the distribution function of the atoms in the crystals or that of the average spin orientation in magnetic substances. More abstract symmetry of wave function is relevant to superconductivity and the $\lambda$-transition of liquid helium. It is generally observed that one or more of the symmetry elements disappear as the substance undergoes the phase transition. The symmetry change is thus a general characteristic of phase transitions.[8] In fact, Landau theory of the phase transitions of the second kind connects the symmetry change with the thermodynamics of the phase transition through appropriate definition of the order parameters. If there is no change in the symmetry of the crystal, how can one distinguish one phase from the other? One cannot tell one phase from the other from the atomic distribution function alone because there is no qualitative difference between the distribution functions of the two phases. A question thus arises as to whether the two phases are really different from each other.

From the calorimetric point of view, the phase transition in TCD is characterized by a sharp peak of the heat capacity.[9,10] The anomalous heat capacity increases symmetrically from both sides of the transition point. This has been recognized as a distinguishing feature of the two-dimensional phase transition. A small isothermal increment of the enthalpy (33.0 J mol$^{-1}$ or 3.5% of the total transition enthalpy) was observed at the very transition temperature of $x$=2.00.[9] Thus, the phase transition occurs gradually but is of the first-order nature. These observations suggest formal similarity of the transition in TCD with vaporization of a typical liquid. Thus the liquid and vapor have the same continuous translational symmetry. Below the critical pressure, the vaporization is, of course, a first-order transition. Far below the critical point, there is no gradual increase of enthalpy in the isobaric process both below and above the vaporization temperature. Only the latent heat of vaporization dominates in that process. However, gradual increase of the enthalpy appears as the critical pressure is approached. At the critical point the isothermal change of enthalpy disappears and the heat capacity at the critical pressure diverges strongly. The region beyond the critical point is called supercritical. Here, the heat capacity as a function of temperature will be still large but remains finite. If the analogy between the phase transition in TCD and vaporization of liquid is something more than superficial, one should expect existence of a critical point at an appropriate value of some external parameter of the TCD crystal. In the present study, we have chosen the hydrogen-deuterium isotopic composition as the adjustable "external" parameter and made heat capacity measurement of the mixed crystals of $SnCl_2(H_2O)_x(D_2O)_{2-x}$ for $x$=2.00, 1.97, 1.75, 1.50, 0.96, 0.50, 0.25, and 0.03.

High resolution measurements of the heat capacity including that of the crystals aged for four years have established that the critical composition does really exist near $x$=1.50. The phase transition in TCD provides thus an example of a new class of solid state phase transition for which there is no concomitant

† Present address: Sumitomo Electric Industries Ltd., Osaka 541.

change of the symmetry of the crystal. It should be mentioned that the dimer model of Salinas and Nagle[11] which gives a logarithmic singularity of heat capacity at the transition point $T_c$ seems to have a similar property in that the symmetry of the dimer distribution is the same for $T>T_c$ as for $T<T_c$. A relevant problem of the difficulty of defining the order parameter for a certain class of the dimer lattice was first pointed out by Kasteleyn.[12]

Another aspect of interest of TCD crystal is that the anomalous heat capacity has an appreciable magnitude even at a lower temperature where the motion of the hydrogen atom is so slow that it falls out of thermal equilibrium when the temperature is varied at a typical rate of the calorimetric experiment.[10] The temperature at which the average lifetime of the proton (or deuteron) configuration is equal to the time required for the heat capacity measurement, *i.e.*, the temperature where the calorimetric Deborah number[13] is equal to unity, is called the glass transition temperature $T_g$. Below $T_g$ only the vibrational degree of the crystal is active and contributes to the observed heat capacity. This is a particularly fortunate property of the crystal, because it leads to unambiguous determination of the lattice heat capacity. Occurrence of the glass transition in TCD is intimately related to the structure of the hydrogen-bond network of the crystal. The network structure is such that the hydrogen atoms can change their positions without violating the ice conditions if eight of them move in unison.[10,14] A very different behavior is observed in copper formate tetrahydrate, a similar hydrate crystal with layer structure, in which the ice condition prohibits redistribution of finite number of the hydrogen atoms in the low-temperature phase. The anomalous heat capacity is essentially zero below $T_c$ because the ordering is complete in the whole range of the low-temperature phase. It has been pointed out previously that Bjerrum and ionic defects can have only minor effect that scarcely affects the bulk thermodynamic properties of the copper formate tetrahydrate crystal, although they may be responsible to the dielectric dispersion in the low temperature phase.[15] In the present study the isotope effect on the glass transition in TCD has also been investigated by the heat capacity measurement. It will be shown that the relaxational properties depend on the isotopic composition in a monotonous way. The experimental result presented in this paper will be analysed in the subsequent paper[16] in terms of the general consideration discussed above.

## Experimental

*Sample Preparation.* The single crystals of solid solution of TCD and DTCD were prepared in the following manner. Commercial TCD (extra pure grade from Wakō Pure Chemical Co., Ltd.) was first dehydrated by evacuation for a week. The extent of dehydration was determined by measurement of the weight loss. An appropriate amount of mixture of normal and 99.75% heavy water (E. Merck) having desired composition was added to the dehydrated crystal together with a small quantity of normal or deuterated hydrochloric acid. The slurry was heated to about 45 °C in a closed glass vessel giving a clear solution and cooled slowly after addition of a small piece of single crystal. The crystal was grown in the water bath thermostatted by the proportional controller (within $\pm 10$ mK) for a month. The sample for the calorimetry was cut from a large single crystal, shaped into a cylinder with 25 mm diameter and 40 mm height, and enclosed in a calorimeter cell under atmosphere of helium. All the six single crystals having different isotopic composition were prepared in the same manner.

*Determination of the Isotopic Composition.* The $H_2O$ concentration in $SnCl_2(H_2O)_{0.96}(D_2O)_{1.04}$ was determined by means of the quantitative absorption intensity measurements of the proton magnetic resonance by use of the high resolution NMR spectrometer (Varian 60). Several mixtures of $D_2O$ and $H_2O$ having different compositions were used as standards for making the calibration curve. The isotopic mixture of water was collected into the NMR tube by vacuum distillation from the calorimetric crystal after completion of the heat capacity measurement. The error in the determination of the deuterium content was estimated to be $\pm 2\%$ from the scatter in the calibration. The mole ratio of $H_2O$ and $D_2O$ in solid solution thus determined agreed with that of the initial mixture. The other solid solutions were assumed to have the same isotopic composition as the slurry.

*Calorimeter.* The design and construction of the high resolution calorimeter used in the present work was described in detail elsewhere.[17] One of the feature of the adiabatic calorimeter is that it is equipped with two thermometers, that is, a platinum resistance thermometer and a thermistor-thermometer. The former is employed to determine heat capacity with ordinary resolution ($\Delta T \approx 1$—2 K) and the inaccuracy and the imprecision of the heat capacity measurement by use of the platinum resistance thermometer is less than $\pm 0.1$ and $\pm 0.05\%$,[18] respectively, between 50 and 275 K. The latter, the thermistor-thermometer, is essential for high resolution measurement with the temperature step of 10—20 mK. The temperature resolution attained by this thermometer was about 3 μK at 220 K. Meticulously careful attention had to be paid to the adiabatic control in order to exploit the good temperature resolution of the thermistor-thermometer. When the control was left undisturbed, the cell temperature remained constant within 0.3 mK over a period of 24 h. Temperature steps as small as 5 mK could be attained without introducing unduely large imprecision in the result. The performance of the calorimeter was improved by several modifications made since the previous publication of the apparatus. Some of them are briefly described here.

i) Use of an indium O-ring facilitates the vacuum-tight closure of the calorimeter cell.

ii) In order to ease the procedure of assembling the calorimeter cell especially in the dry-box, two gold electric contacts were attached to the hermetic seal as the terminal for the calorimeter-heater-leads.

iii) In order to decrease the heat transfer to the calorimeter cell by conduction along the electrical leads, one of the thermocouple junctions, which was previously located between the calorimeter cell and bottom cone, was fixed to the inner jacket. The copper leads of the two thermometers were replaced by the constantan leads with smaller thermal conductivity.

iv) The significant temperature drift was caused by the stray E.M.F. induced at the terminal of the thermocouple-lead in the previous high resolution measurement. The stray E.M.F. was reduced by decreasing the number of binding-post between the calorimeter and the microvolt amplifier.

TABLE 1. SUMMARY OF SOLID SOLUTIONS AND AGING PERIOD

| Abbreviation | Formula | $t$/month[a)] |
|---|---|---|
| $x=2.00$ | $SnCl_2(H_2O)_{2.00}$ | 3 |
| $x=1.97$ | $SnCl_2(H_2O)_{1.97}(D_2O)_{0.03}$ | 4 |
| $x=1.75$ | $SnCl_2(H_2O)_{1.75}(D_2O)_{0.25}$ | 4 |
| $x=1.50$ | $SnCl_2(H_2O)_{1.50}(D_2O)_{0.50}$ | 7 |
| $x=0.96$ | $SnCl_2(H_2O)_{0.96}(D_2O)_{1.04}$ | 1 |
| $x=0.96$(II) | $SnCl_2(H_2O)_{0.96}(D_2O)_{1.04}$ | 24 |
| $x=0.50$ | $SnCl_2(H_2O)_{0.50}(D_2O)_{1.50}$ | 4 |
| $x=0.50$(II) | $SnCl_2(H_2O)_{0.50}(D_2O)_{1.50}$ | 10 |
| $x=0.25$ | $SnCl_2(H_2O)_{0.25}(D_2O)_{1.75}$ | 1 |
| $x=0.03$ | $SnCl_2(H_2O)_{0.03}(D_2O)_{1.97}$ | 1 |
| $x=0.03$(II) | $SnCl_2(H_2O)_{0.03}(D_2O)_{1.97}$ | 48 |

a) Time elapsed before starting the measurement after the preparation of the crystal.

v) The ASL AC double bridge works adequately when the resistance ratio ($n_A$) is between 0.2 and 0.8. Previously, we used two home-made standard resistors (6.238453 and 0.390430 Ω) and a commercial one of 100 Ω (Shimadzu Electrical Measuring Instruments Co., Ltd.). The first resistors were replaced by three card-type precision resistors (10, 1, 0.1 Ω, General Radio Company) resulting in ample overlap between the intervals of the recommended ratio value. This modifications did not influence the temperature scale because the new resistors were calibrated against the 100 Ω resistor which remained as before.

vi) The maximum temperature coefficient of the card-type standard resistor has been stated ±20 ppm/K by the manufacturer. The improved thermostat was constructed, which consisted of the double-walled-aluminium box temperature-regulated by proportional controllers. The temperature was kept constant within ±50 mK.

vii) The effect of the self-heating is corrected more reproducibly by monitoring the accurate power dissipated in the thermometer. For this purpose the bridge carrier voltage was measured by an AC voltmeter (Yokogawa Electric Works Ltd.).

viii) Temperature constancy of the bridge components was found to be essential for the high resolution measurement especially in the vicinity of critical points where thermal equilibrium is reached very sluggishly. In order to stabilize the temperature of the bridge components (two 1 kΩ resistors for the fixed arms and a seven-decade 111.11110 kΩ variable resistor) against the change of the room temperature, they were housed in an air thermostat. The temperature of the thermostat was regulated within ±0.1 K by a controller equipped with a thermistor throughout a series of heat capacity measurements. Temperature gradient in the air thermostat was minimized by a fan driven by a remote motor through a flexible torque transmitter.

*Heat Capacity Measurements.* The heat capacity measurements were performed on crystals of seven different compositions in addition to $x=2.00$ already reported. Table 1 summarizes the isotopic composition of the samples and the time elapsed between preparation of the crystal and the heat capacity measurement. The abbreviatiated designation for each of the solid solutions is also given there.

In all of the isotopic compositions studied, the heat capacity behaved anomalously in two temperature regions. One is around 220—230 K region and is due to the order-disorder change of proton (deuteron) in the hydrogen bonding network. The other is a relaxational anomaly (glass transition) around

TABLE 2. MOLAR HEAT CAPACITY OF $SnCl_2(H_2O)_{2.00}$

| $T$/K | $C_p$ / J K$^{-1}$ mol$^{-1}$ | $T$/K | $C_p$ / J K$^{-1}$ mol$^{-1}$ | $T$/K | $C_p$ / J K$^{-1}$ mol$^{-1}$ |
|---|---|---|---|---|---|
| 216.009 | 149.79 | 217.866 | 182.97 | 218.886 | 155.67 |
| 216.081 | 149.89 | 217.885 | 186.93 | 218.911 | 155.33 |
| 216.152 | 150.23 | 217.903 | 191.27 | 218.965 | 154.78 |
| 216.224 | 150.51 | 217.921 | 197.99 | 218.988 | 154.62 |
| 216.295 | 150.78 | 217.938 | 208.20 | 219.014 | 154.31 |
| 216.354 | 151.06 | 217.955 | 224.55 | 219.042 | 153.99 |
| 216.402 | 151.15 | 217.970 | 253.90 | 219.070 | 153.71 |
| 216.438 | 151.48 | 217.984 | 305.39 | 219.098 | 153.53 |
| 216.467 | 151.53 | | | 219.126 | 153.38 |
| 216.499 | 151.62 | 1st order region | | 219.154 | 153.23 |
| 216.531 | 151.79 | | | 219.182 | 153.08 |
| 216.563 | 151.97 | 218.022 | 236.73 | 219.210 | 152.94 |
| 216.595 | 152.11 | 218.038 | 216.23 | 219.238 | 152.72 |
| 216.627 | 152.22 | 218.055 | 204.46 | 219.266 | 152.58 |
| 216.659 | 152.58 | 218.072 | 196.40 | 219.294 | 152.61 |
| 216.691 | 152.64 | 218.090 | 190.49 | 219.322 | 152.43 |
| 216.723 | 152.79 | 218.108 | 186.12 | 219.350 | 152.28 |
| 216.755 | 152.99 | 218.127 | 182.72 | 219.378 | 151.93 |
| 216.786 | 153.19 | 218.146 | 179.78 | 219.406 | 151.94 |
| 216.818 | 153.41 | 218.165 | 177.52 | 219.438 | 151.88 |
| 216.850 | 153.74 | 218.184 | 175.40 | 219.473 | 151.77 |
| 216.881 | 153.69 | 218.203 | 173.65 | 219.508 | 151.41 |
| 216.913 | 154.17 | 218.222 | 172.03 | 219.542 | 151.40 |
| 216.945 | 154.28 | 218.241 | 170.61 | 219.577 | 151.21 |
| 216.976 | 154.66 | 218.261 | 169.14 | 219.613 | 151.13 |
| 217.008 | 154.95 | 218.280 | 168.34 | 219.650 | 150.78 |
| 217.039 | 155.09 | 218.300 | 167.30 | 219.690 | 150.68 |
| 217.071 | 155.07 | 218.321 | 166.64 | 219.730 | 150.55 |
| 217.102 | 155.58 | 218.342 | 165.78 | 219.772 | 150.39 |
| 217.134 | 155.85 | 218.362 | 165.06 | 219.814 | 150.25 |
| 217.165 | 156.22 | 218.382 | 164.15 | 219.858 | 150.19 |
| 217.197 | 156.65 | 218.402 | 163.55 | 219.904 | 149.77 |
| 217.228 | 156.90 | 218.422 | 162.88 | 219.951 | 149.98 |
| 217.259 | 157.38 | 218.442 | 162.49 | 220.140 | 149.32 |
| 217.291 | 157.68 | 218.462 | 161.83 | 220.490 | 148.56 |
| 217.322 | 158.19 | 218.482 | 161.32 | 220.885 | 147.72 |
| 217.353 | 158.54 | 218.502 | 160.93 | 221.309 | 147.11 |
| 217.384 | 159.11 | 218.522 | 160.38 | 221.734 | 146.62 |
| 217.415 | 159.64 | 218.543 | 160.28 | 222.159 | 146.19 |
| 217.446 | 160.21 | 218.563 | 159.93 | 222.585 | 146.09 |
| 217.477 | 160.79 | 218.583 | 159.93 | 223.012 | 145.57 |
| 217.507 | 161.20 | 218.603 | 159.47 | 223.440 | 144.79 |
| 217.537 | 162.14 | 218.624 | 158.99 | | |
| 217.566 | 163.07 | 218.644 | 158.63 | | |
| 217.596 | 163.90 | 218.665 | 158.24 | | |
| 217.625 | 164.94 | 218.686 | 157.94 | | |
| 217.653 | 165.26 | 218.707 | 157.60 | | |
| 217.705 | 168.28 | 218.729 | 157.31 | | |
| 217.729 | 169.63 | 218.750 | 156.85 | | |
| 217.753 | 171.31 | 218.772 | 156.65 | | |
| 217.778 | 173.02 | 218.794 | 156.33 | | |
| 217.803 | 175.10 | 218.817 | 156.22 | | |
| 217.826 | 177.86 | 218.840 | 155.86 | | |
| 217.847 | 180.27 | 218.863 | 155.76 | | |

TABLE 3. MOLAR HEAT CAPACITY OF $SnCl_2(H_2O)_{1.50}(D_2O)_{0.50}$

| $T$/K | $C_p$/J K$^{-1}$ mol$^{-1}$ | $T$/K | $C_p$/J K$^{-1}$ mol$^{-1}$ | $T$/K | $C_p$/J K$^{-1}$ mol$^{-1}$ | $T$/K | $C_p$/J K$^{-1}$ mol$^{-1}$ | $T$/K | $C_p$/J K$^{-1}$ mol$^{-1}$ |
|---|---|---|---|---|---|---|---|---|---|
| 198.46 | 136.63 | 163.05 | 121.20 | 220.445 | 156.75 | 221.785 | 221.11 | 222.494 | 165.36 |
| 199.70 | 137.64 | 164.14 | 121.69 | 220.476 | 157.03 | 221.796 | 229.21 | 222.509 | 165.34 |
| 200.95 | 138.03 | 165.23 | 122.19 | 220.512 | 156.72 | 221.807 | 238.83 | 222.525 | 164.46 |
| 202.34 | 138.98 | 166.31 | 122.61 | 220.548 | 157.48 | 221.818 | 250.57 | 222.540 | 164.57 |
| 203.83 | 139.63 | 167.40 | 123.09 | 220.584 | 157.46 | 221.828 | 266.17 | 222.556 | 163.99 |
| 205.26 | 140.29 | 168.46 | 123.63 | 220.619 | 157.86 | 221.838 | 284.06 | 222.572 | 163.70 |
| 206.69 | 141.08 | 169.54 | 124.12 | 220.653 | 157.78 | 221.847 | 306.45 | 222.588 | 163.98 |
| 208.15 | 141.87 | 170.81 | 124.65 | 220.687 | 158.27 | 221.856 | 344.73 | 222.603 | 163.24 |
| 209.59 | 142.72 | 172.38 | 125.35 | 220.721 | 158.46 | 221.863 | 396.40 | 222.619 | 162.81 |
| 210.99 | 143.60 | 174.00 | 125.99 | 220.755 | 158.64 | 221.870 | 465.68 | 222.635 | 162.57 |
| 212.38 | 144.47 | 175.63 | 126.95 | 220.789 | 159.01 | 221.876 | 571.29 | 222.651 | 162.27 |
| 213.76 | 145.53 | 173.43 | 125.82 | 220.823 | 159.39 | 221.881 | 459.08 | 222.667 | 162.10 |
| 215.15 | 146.67 | 175.28 | 126.63 | 220.852 | 159.26 | 221.888 | 422.80 | 222.684 | 161.89 |
| 216.53 | 148.09 | 177.12 | 127.45 | 220.884 | 159.72 | 221.895 | 382.22 | 222.700 | 161.38 |
| 217.93 | 149.86 | 178.95 | 128.24 | 220.917 | 160.07 | 221.903 | 357.60 | 222.716 | 161.48 |
| 219.42 | 153.64 | 180.77 | 129.07 | 220.950 | 160.23 | 221.912 | 329.33 | 222.732 | 161.22 |
| 220.68 | 159.19 | 182.68 | 129.91 | 220.983 | 161.01 | 221.921 | 304.43 | 222.748 | 161.04 |
| 221.94 | 202.54 | 184.69 | 130.77 | 221.015 | 161.29 | 221.930 | 287.57 | 222.765 | 160.98 |
| 223.17 | 158.24 | 186.68 | 131.68 | 221.047 | 161.60 | 221.940 | 268.62 | 222.781 | 160.80 |
| 224.49 | 153.40 | 188.67 | 132.61 | 221.077 | 162.00 | 221.951 | 255.16 | 222.797 | 160.15 |
| 225.77 | 151.26 | 190.63 | 133.44 | 221.106 | 162.60 | 221.961 | 242.62 | 222.814 | 160.05 |
| 227.13 | 149.98 | 192.59 | 134.25 | 221.135 | 162.85 | 221.973 | 232.62 | 222.830 | 161.44 |
| 228.48 | 149.32 | 194.54 | 135.37 | 221.163 | 163.44 | 221.982 | 223.67 | 222.847 | 160.60 |
| 229.84 | 149.05 | 196.48 | 136.11 | 221.191 | 163.81 | 221.993 | 218.73 | 222.864 | 159.53 |
| | | 198.40 | 136.95 | 221.219 | 164.27 | 222.006 | 214.50 | 222.882 | 159.62 |
| | | 200.16 | 137.86 | 221.247 | 164.70 | 222.018 | 208.52 | 222.899 | 159.49 |
| | | 201.74 | 138.73 | 221.273 | 165.54 | 222.030 | 203.10 | 222.917 | 159.00 |
| 125.50 | 101.07 | 203.15 | 139.34 | 221.297 | 166.06 | 222.043 | 200.24 | 222.935 | 159.19 |
| 126.55 | 101.57 | 204.40 | 139.93 | 221.314 | 165.84 | 222.056 | 195.20 | 222.953 | 159.09 |
| 127.64 | 102.12 | 205.64 | 140.54 | 221.334 | 166.39 | 222.069 | 193.12 | 222.967 | 158.42 |
| 128.82 | 102.67 | 206.79 | 141.30 | 221.353 | 167.38 | 222.082 | 190.70 | 222.986 | 158.40 |
| 130.19 | 103.27 | 207.85 | 141.89 | 221.372 | 167.75 | 222.096 | 188.47 | 223.004 | 158.39 |
| 131.36 | 103.96 | 208.89 | 142.43 | 221.390 | 168.63 | 222.109 | 186.51 | 223.023 | 158.24 |
| 132.60 | 104.52 | 209.87 | 143.09 | 221.409 | 169.32 | 222.123 | 185.04 | 223.042 | 157.63 |
| 133.83 | 105.09 | 210.78 | 143.45 | 221.426 | 169.89 | 222.133 | 182.32 | 223.058 | 157.84 |
| 135.06 | 105.66 | | | 221.444 | 170.50 | 222.147 | 181.06 | 223.078 | 157.88 |
| 136.28 | 106.25 | 215.583 | 147.06 | 221.461 | 171.10 | 222.161 | 179.74 | 223.098 | 157.97 |
| 137.50 | 106.78 | 216.128 | 147.60 | 221.478 | 172.00 | 222.175 | 178.39 | 223.118 | 157.91 |
| 138.71 | 107.39 | 216.593 | 148.11 | 221.495 | 172.80 | 222.189 | 178.27 | 223.139 | 157.53 |
| 139.91 | 108.38 | 217.046 | 148.62 | 221.512 | 173.89 | 222.202 | 176.64 | 223.162 | 157.25 |
| 141.12 | 108.59 | 217.470 | 149.16 | 221.528 | 175.26 | 222.217 | 175.98 | 223.184 | 157.52 |
| 142.32 | 109.13 | 217.845 | 149.39 | 221.543 | 176.12 | 222.231 | 174.95 | 223.206 | 157.16 |
| 143.50 | 109.43 | 218.144 | 150.07 | 221.559 | 176.07 | 222.245 | 174.39 | 223.228 | 157.15 |
| 144.70 | 110.21 | 218.399 | 150.52 | 221.573 | 177.77 | 222.259 | 173.32 | 223.252 | 157.00 |
| 145.89 | 110.77 | 218.640 | 150.96 | 221.588 | 178.44 | 222.273 | 172.35 | 223.278 | 156.75 |
| 147.08 | 111.28 | 218.867 | 151.46 | 221.602 | 179.83 | 222.288 | 171.91 | 223.303 | 156.68 |
| 148.25 | 111.80 | 219.075 | 151.83 | 221.616 | 181.38 | 222.302 | 171.58 | 223.329 | 156.51 |
| 149.44 | 112.26 | 219.276 | 152.36 | 221.630 | 183.55 | 222.317 | 170.58 | 223.355 | 156.61 |
| 150.62 | 112.83 | 219.468 | 152.83 | 221.644 | 183.52 | 222.331 | 170.10 | 223.382 | 156.06 |
| 151.81 | 113.27 | 219.652 | 153.42 | 221.658 | 185.32 | 222.346 | 169.22 | 223.409 | 156.25 |
| 152.98 | 113.77 | 219.813 | 153.90 | 221.671 | 187.52 | 222.360 | 169.08 | 223.438 | 155.86 |
| 154.15 | 114.31 | 219.950 | 154.27 | 221.685 | 189.57 | 222.375 | 168.17 | 223.468 | 155.97 |
| 155.30 | 115.45 | 220.062 | 154.74 | 221.698 | 192.24 | 222.390 | 167.94 | 223.498 | 155.63 |
| 156.42 | 117.98 | 220.141 | 155.12 | 221.711 | 194.54 | 222.404 | 167.49 | 223.528 | 155.85 |
| 157.54 | 118.87 | 220.205 | 155.43 | 221.724 | 197.79 | 222.419 | 167.25 | 223.558 | 155.30 |
| 158.64 | 119.21 | 220.260 | 155.57 | 221.736 | 200.65 | 222.434 | 166.41 | 223.588 | 155.43 |
| 159.75 | 119.71 | 220.311 | 155.94 | 221.749 | 204.78 | 222.449 | 166.43 | 223.619 | 155.28 |
| 160.86 | 120.38 | 220.357 | 156.20 | 221.761 | 212.19 | 222.464 | 166.04 | 223.650 | 155.15 |
| 161.96 | 120.74 | 220.402 | 156.51 | 221.773 | 214.91 | 222.479 | 165.03 | 223.682 | 155.15 |

TABLE 3. Continued

| $T$/K | $C_p$/J K$^{-1}$ mol$^{-1}$ | $T$/K | $C_p$/J K$^{-1}$ mol$^{-1}$ | $T$/K | $C_p$/J K$^{-1}$ mol$^{-1}$ | $T$/K | $C_p$/J K$^{-1}$ mol$^{-1}$ |
|---|---|---|---|---|---|---|---|
| 223.714 | 155.00 | 58.99 | 55.72 | 238.93 | 149.63 | 26.73 | 20.17 |
| 223.748 | 154.87 | 60.35 | 56.99 | 240.23 | 149.82 | 27.80 | 21.49 |
| 223.783 | 154.73 | 61.80 | 58.30 | 241.51 | 150.13 | 28.81 | 22.71 |
| 223.819 | 154.46 | 63.35 | 59.68 | 242.87 | 150.22 | 29.75 | 23.85 |
| 223.855 | 154.39 | 64.87 | 61.00 | 244.29 | 150.70 | 30.74 | 25.04 |
| 223.891 | 154.44 | 66.32 | 62.28 | 245.71 | 150.83 | 31.86 | 26.40 |
| 223.931 | 154.24 | 67.85 | 63.56 | 247.13 | 151.25 | 32.96 | 27.76 |
| 223.976 | 153.88 | 69.42 | 64.92 | 248.54 | 151.52 | 33.96 | 28.94 |
| 224.020 | 153.77 | 70.97 | 66.21 | 250.05 | 151.91 | 34.92 | 30.06 |
| 224.065 | 153.81 | 72.49 | 67.47 | 251.68 | 152.33 | 35.88 | 31.22 |
| 224.111 | 153.92 | 73.96 | 68.69 | 253.31 | 152.80 | 36.79 | 32.24 |
| 224.158 | 153.79 | 75.54 | 69.90 | 254.92 | 153.20 | 37.74 | 33.32 |
| 224.213 | 153.45 | 77.21 | 71.21 | 256.54 | 153.46 | 38.71 | 34.42 |
| 224.274 | 153.50 | 78.84 | 72.45 | 258.15 | 153.94 | 39.64 | 35.44 |
| 224.335 | 153.28 | | | 259.85 | 154.40 | 40.62 | 36.55 |
| 224.397 | 153.40 | | | 261.46 | 154.81 | 41.67 | 37.74 |
| 224.457 | 152.72 | 80.44 | 73.67 | 263.24 | 155.32 | 42.69 | 38.87 |
| 224.522 | 152.92 | 82.01 | 74.70 | 265.03 | 155.82 | 43.77 | 40.07 |
| 224.591 | 153.01 | 83.56 | 75.96 | | | 44.92 | 41.31 |
| 224.662 | 152.67 | 84.98 | 77.00 | | | 46.01 | 42.54 |
| 224.731 | 152.76 | 86.57 | 78.08 | 266.81 | 156.35 | 47.08 | 43.67 |
| 224.805 | 152.44 | 88.17 | 79.12 | 268.59 | 156.87 | 48.15 | 44.82 |
| 224.880 | 152.40 | 89.86 | 80.27 | 270.47 | 157.37 | | |
| 224.931 | 152.69 | 91.52 | 81.42 | 272.53 | 158.08 | | |
| 224.981 | 152.44 | 93.18 | 82.45 | 274.64 | 158.61 | | |
| 225.081 | 152.30 | 94.79 | 83.56 | 276.75 | 159.30 | | |
| 225.203 | 152.17 | 96.36 | 84.52 | 278.85 | 160.06 | | |
| 225.325 | 152.10 | 97.92 | 85.58 | 280.93 | 160.56 | | |
| 225.473 | 152.08 | 99.45 | 86.48 | 283.01 | 161.16 | 49.22 | 46.00 |
| 225.643 | 151.48 | 101.03 | 87.51 | 285.08 | 161.77 | 50.48 | 47.31 |
| 225.861 | 151.60 | 102.63 | 88.45 | 287.15 | 162.55 | 51.91 | 48.84 |
| 226.166 | 151.01 | 104.22 | 89.41 | 289.21 | 163.21 | 53.31 | 50.20 |
| 226.517 | 150.16 | 105.78 | 90.37 | 291.23 | 164.07 | 54.75 | 51.68 |
| 226.868 | 150.00 | 107.34 | 91.23 | 293.28 | 164.41 | 56.23 | 53.10 |
| 227.219 | 149.90 | 108.88 | 92.17 | 295.39 | 165.01 | 57.67 | 54.48 |
| 227.661 | 149.72 | 110.41 | 93.01 | 297.60 | 165.80 | 59.06 | 55.77 |
| 228.193 | 149.44 | 111.91 | 93.81 | 299.88 | 166.63 | | |
| 228.771 | 149.27 | 113.42 | 94.71 | 302.24 | 167.64 | | |
| 229.385 | 148.74 | 114.95 | 95.52 | | | | |
| 229.992 | 148.95 | 116.54 | 96.28 | | | 130.04 | 103.22 |
| 230.608 | 148.95 | 118.09 | 97.24 | | | 131.70 | 104.06 |
| 231.240 | 148.89 | 119.63 | 98.04 | 13.14 | 4.87 | 133.51 | 104.89 |
| 231.967 | 148.85 | 121.18 | 98.83 | 13.75 | 5.48 | 135.41 | 105.80 |
| 232.774 | 148.89 | 122.70 | 99.66 | 14.32 | 6.00 | 137.29 | 106.67 |
| 233.581 | 149.00 | 124.22 | 100.38 | 15.18 | 6.88 | 139.22 | 107.53 |
| 234.388 | 148.99 | 125.72 | 101.20 | 16.35 | 7.97 | 141.19 | 108.43 |
| 235.195 | 149.04 | | | 17.18 | 8.94 | 143.15 | 109.37 |
| 236.001 | 149.21 | | | 18.00 | 9.85 | 145.15 | 110.38 |
| 236.801 | 149.22 | | | 18.77 | 10.74 | 147.08 | 111.26 |
| 237.605 | 149.36 | 227.43 | 149.82 | 19.46 | 11.54 | 148.99 | 112.08 |
| 238.409 | 149.62 | 228.84 | 149.34 | 20.19 | 12.40 | 150.84 | 112.96 |
| | | 230.27 | 149.09 | 20.94 | 13.25 | 152.60 | 114.84 |
| 239.33 | 149.27 | 231.45 | 148.99 | 21.75 | 14.20 | 154.40 | 117.15 |
| 240.38 | 149.78 | 232.63 | 148.98 | 22.62 | 15.23 | 156.24 | 117.95 |
| 241.49 | 150.00 | 233.81 | 148.95 | 23.42 | 16.17 | 158.07 | 118.62 |
| 242.70 | 149.71 | 235.05 | 149.11 | 24.18 | 17.07 | 159.98 | 119.73 |
| 243.90 | 150.81 | 236.34 | 149.33 | 24.96 | 18.05 | 162.03 | 120.61 |
| | | 237.64 | 149.38 | 25.77 | 19.07 | 164.24 | 121.63 |

TABLE 4. MOLAR HEAT CAPACITY OF $SnCl_2(H_2O)_{0.03}(D_2O)_{1.97}$

| $T$/K | $C_p$/J K$^{-1}$ mol$^{-1}$ | $T$/K | $C_p$/J K$^{-1}$ mol$^{-1}$ | $T$/K | $C_p$/J K$^{-1}$ mol$^{-1}$ | $T$/K | $C_p$/J K$^{-1}$ mol$^{-1}$ |
|---|---|---|---|---|---|---|---|
| 232.482 | 172.83 | 234.646 | 231.07 | 236.497 | 174.39 | 234.550 | 225.42 |
| 232.541 | 173.06 | 234.668 | 230.04 | 236.564 | 174.19 | 234.582 | 229.23 |
| 232.596 | 173.28 | 234.694 | 229.89 | 236.641 | 173.90 | 234.602 | 230.67 |
| 232.651 | 173.52 | 234.720 | 228.70 | 236.719 | 173.61 | 234.618 | 228.64 |
| 232.705 | 173.71 | 234.746 | 227.18 | 236.799 | 173.35 | 234.634 | 227.56 |
| 232.755 | 173.94 | 234.774 | 224.62 | 236.871 | 173.14 | 234.651 | 228.42 |
| 232.804 | 174.16 | 235.043 | 198.62 | 236.933 | 172.94 | 234.668 | 230.76 |
| 232.853 | 174.54 | 235.012 | 200.17 | 237.042 | 172.76 | 234.684 | 231.73 |
| 232.899 | 174.60 | 234.981 | 203.45 | 237.196 | 172.41 | 234.785 | 221.27 |
| 232.946 | 174.77 | 234.950 | 206.25 | 237.350 | 172.01 | 234.809 | 215.92 |
| 232.993 | 175.07 | 234.920 | 209.37 | 237.505 | 171.68 | 234.838 | 213.97 |
| 233.040 | 175.16 | 234.890 | 212.23 | 237.661 | 171.40 | 234.871 | 208.12 |
| 233.086 | 175.64 | 234.861 | 215.70 | 237.817 | 171.11 | 234.904 | 203.25 |
| 233.133 | 177.64 | 234.832 | 219.13 | 237.972 | 170.95 | 234.944 | 200.52 |
| 233.178 | 176.21 | 234.803 | 221.90 | 238.128 | 170.64 | 234.997 | 195.44 |
| 233.223 | 176.39 | 235.074 | 196.48 | 238.283 | 170.43 | 235.066 | 190.00 |
| 233.267 | 176.58 | 235.106 | 194.70 | 238.574 | 170.22 | 235.143 | 185.95 |
| 233.312 | 177.16 | 235.137 | 192.90 | 239.053 | 169.78 | 235.222 | 182.63 |
| 233.356 | 177.57 | 235.169 | 191.69 | 239.586 | 169.37 | 235.319 | 177.05 |
| 233.400 | 177.86 | 235.201 | 190.38 | | | 235.403 | 179.21 |
| 233.444 | 178.36 | 235.233 | 189.46 | | | 235.505 | 177.80 |
| 233.488 | 178.69 | 235.265 | 188.06 | | | 235.616 | 174.81 |
| 233.529 | 179.19 | 235.298 | 187.22 | 222.69 | 156.27 | 235.756 | 173.59 |
| 233.566 | 179.85 | 235.330 | 186.29 | 223.56 | 156.87 | 235.925 | 172.50 |
| 233.604 | 179.80 | 235.363 | 185.46 | 224.44 | 157.48 | 236.122 | 170.64 |
| 233.641 | 180.55 | 235.395 | 184.73 | 225.30 | 157.36 | 236.350 | 169.41 |
| 233.678 | 182.07 | 235.428 | 183.97 | 226.21 | 158.70 | 236.578 | 168.45 |
| 233.715 | 181.70 | 235.462 | 183.31 | 227.15 | 159.51 | 236.858 | 167.49 |
| 233.751 | 182.05 | 235.495 | 182.74 | | | 237.213 | 166.53 |
| 233.788 | 182.57 | 235.529 | 182.20 | | | 237.686 | 165.76 |
| 233.825 | 183.36 | 235.562 | 181.47 | | | 238.254 | 164.95 |
| 233.861 | 183.89 | 235.595 | 181.01 | 225.11 | 157.55 | 238.822 | 164.41 |
| 233.898 | 184.50 | 235.628 | 180.66 | 226.48 | 158.59 | | |
| 233.935 | 185.07 | 235.661 | 180.19 | 227.84 | 159.69 | | |
| 233.969 | 186.47 | 235.694 | 179.87 | 229.19 | 161.03 | | |
| 234.006 | 187.27 | 235.728 | 179.65 | 230.40 | 162.60 | | |
| 234.040 | 188.57 | 235.761 | 179.15 | 231.33 | 163.97 | | |
| 234.072 | 189.70 | 235.794 | 178.44 | 231.901 | 165.76 | | |
| 234.104 | 191.03 | 235.828 | 178.40 | 232.248 | 166.37 | | |
| 234.136 | 192.35 | 235.861 | 178.04 | 232.535 | 167.79 | | |
| 234.168 | 193.82 | 235.896 | 177.82 | 232.764 | 168.50 | | |
| 234.199 | 195.66 | 235.931 | 177.47 | 232.993 | 169.60 | | |
| 234.231 | 197.06 | 235.967 | 177.21 | 233.220 | 170.33 | | |
| 234.262 | 199.05 | 236.002 | 177.10 | 233.447 | 172.78 | | |
| 234.293 | 201.43 | 236.038 | 176.94 | 233.615 | 174.66 | | |
| 234.323 | 204.00 | 236.073 | 176.65 | 233.728 | 175.78 | | |
| 234.354 | 206.89 | 236.110 | 176.41 | 233.842 | 177.46 | | |
| 234.384 | 209.89 | 236.147 | 176.22 | 233.939 | 179.46 | | |
| 234.413 | 213.06 | 236.185 | 176.10 | 234.032 | 182.74 | | |
| 234.443 | 216.19 | 236.223 | 175.79 | 234.120 | 186.51 | | |
| 234.472 | 219.35 | 236.260 | 175.56 | 234.202 | 189.36 | | |
| 234.501 | 222.41 | 236.298 | 175.36 | 234.278 | 194.13 | | |
| 234.529 | 225.09 | 236.336 | 175.16 | 234.353 | 200.52 | | |
| 234.558 | 227.13 | 236.374 | 174.94 | 234.419 | 210.12 | | |
| 234.595 | 229.34 | 236.413 | 174.76 | 234.463 | 216.12 | | |
| 234.628 | 230.27 | 236.451 | 174.50 | 234.514 | 221.63 | | |

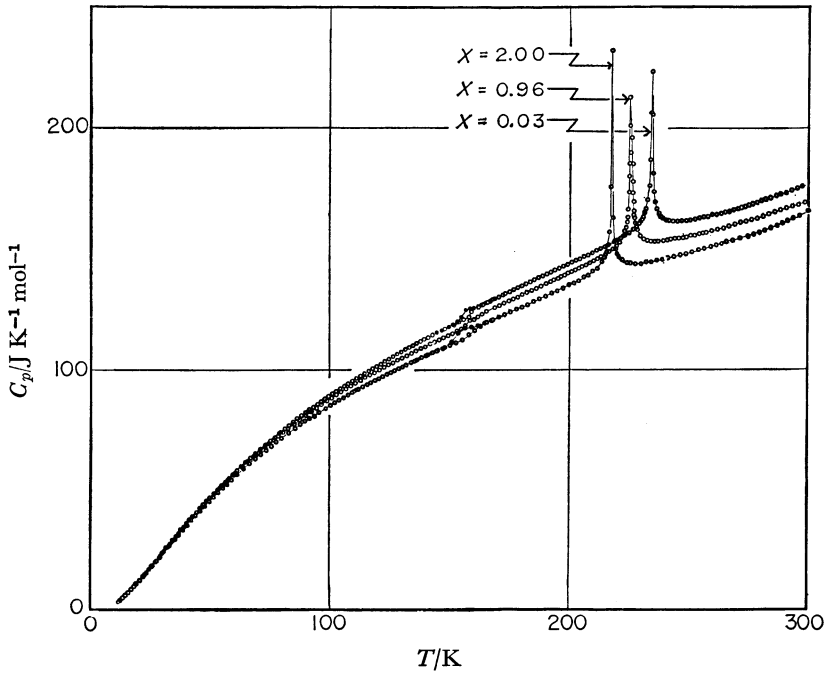


Fig. 1. Heat capacity curves for the samples of $x=2.00$, $x=0.96$, and $x=0.03$.

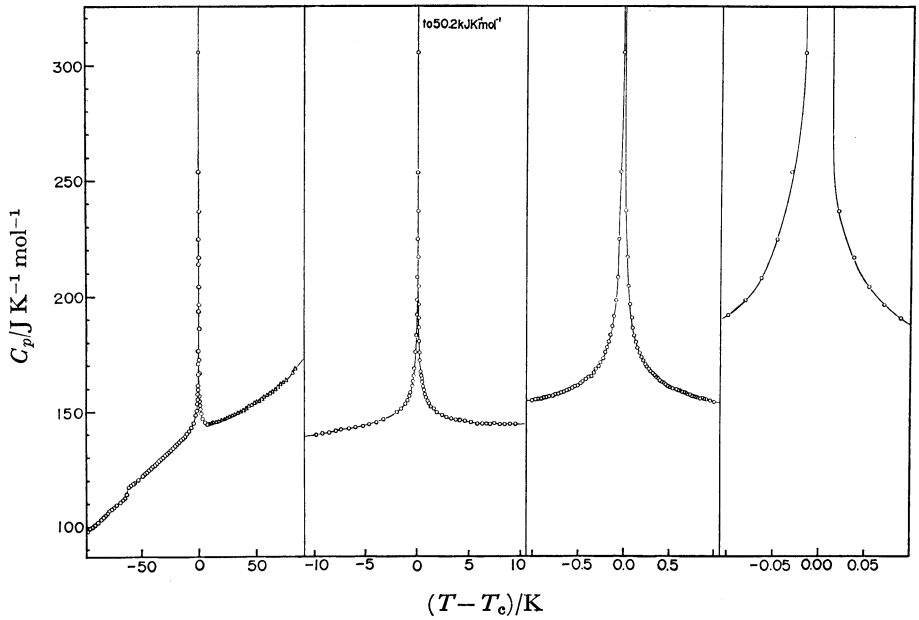


Fig. 2. Heat capacity curves of $x=2.00$ as a function of $(T-T_c)$ in successively expanded scales.

150 K due to loss of equilibrium in rearrangement of protons in that network at the lower temperature. Both anomalies change smoothly with the isotopic composition in their characters including the temperature and the interval of their occurrence. Each measurement was carried out both with ordinary resolution ($\Delta T \approx 1$—3 K) from 11 to 300 K and with high resolution ($\Delta T \approx 10$—50 mK) in the vicinity of the transition temperature. Prior to the high resolution measurement, the transition temperature was located by the measurement with ordinary temperature step. It took about fifteen minutes for all crystals to attain thermal equilibrium after switching off the heater current. Longer time was required to determine the final temperature in the high resolution measurement. Calorimetric operations around the glass transition were performed according to the procedure already reported.[10] Thus the calorimeter was first cooled rapidly to 130 K, some 25 K below the anomalous region. The cooling rate was about 2 K min$^{-1}$. In the measurements in the exothermic region, temperature drifts were followed for 30—60 min after the energy input for heat capacity measurements. These periods were kept constant for a series of measurement. In the endothermic region, heat capacities were measured in the same way as in normal region but by following temperature drift for longer time (2—3 h). Details of the heat capacity measurement for each of the samples are described in the following. The numerical values of the heat capacity are given in Tables 2, 3, and 4 for $x=2.00$, $x=1.50$, and $x=0.03$, respectively. The

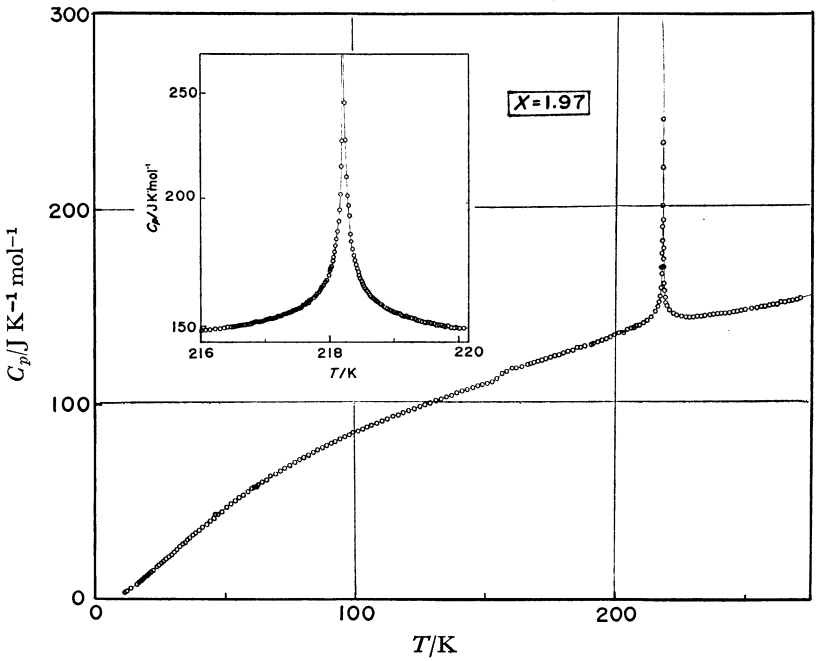


Fig. 3. Heat capacity of $x=1.97$. The inset shows an expanded view close to $T_c$.

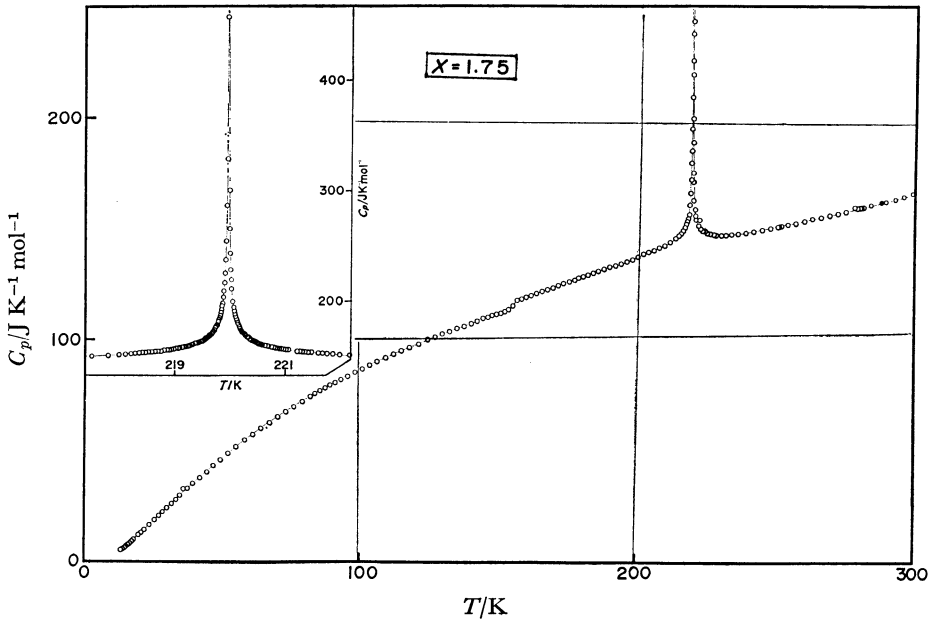


Fig. 4. Heat capacity of $x=1.75$. The inset shows an expanded view close to $T_c$.

complete data of other crystals amounting in number to 2096 are all kept as Document No. 7913 at the Chemical Society of Japan. Figure 1 shows the results of heat capacity measurements of $x=2.00$, $x=0.96$, and $x=0.03$ with ordinary resolutions.

(i) $x=2.00$: The highly symmetrical shape of the anomaly was observed at 218.01 K with a quasi-isothermal absorption of energy amounting to 32.4 J mol$^{-1}$. It is somewhat difficult to distinguish experimentally the small isothermal enthalpy increase (*i.e.* the first-order component) from the very large heat capacity. The first-order component is calorimetrically detected by abrupt increase of large endothermic drift with longer equilibration time and by the steep rise in the enthalpy or entropy curve plotted against temperature (see Ref. 16). The present measurements are precise enough to detect the quasi first-order component. In Fig. 2 the heat capacities are plotted as a function of $(T-T_c)$ in successively expanded scales.

(ii) $x=0.03$: This crystal exhibited no first-order component. The heat capacity curve is rounded at the peak temperature (234.64 K). The anomalous heat capacity was broader than those found in any other crystal and the maximum value of the peak, 220 J K$^{-1}$ mol$^{-1}$, is the smallest in the series of the mixed crystals.

(iii) $x=1.97$: The phase transition occurred at 218.22 K. A quasi-isothermal absorption of energy was found around $\pm 15$ mK of the peak temperature. In this region the equilibration time increased by a factor of 4—6 with a sudden increase

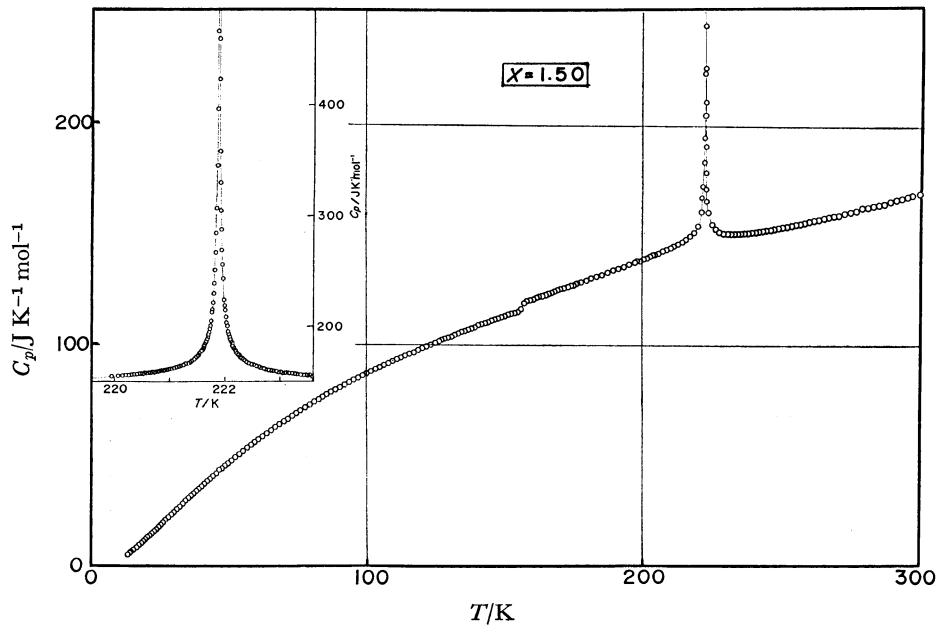


Fig. 5. Heat capacity of $x=1.50$. The inset shows an expanded view close to $T_c$.

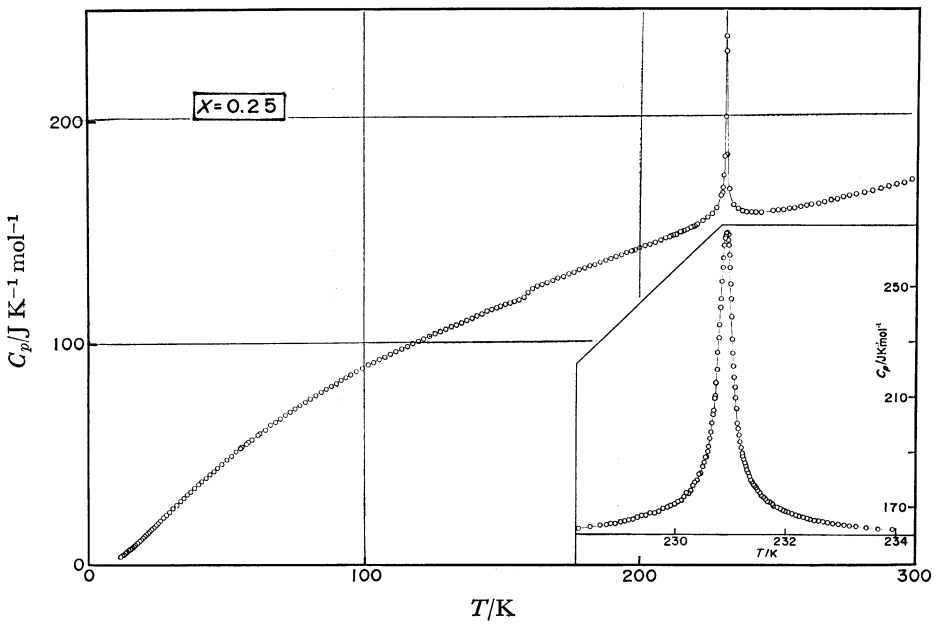


Fig. 6. Heat capacity of $x=0.25$. The inset shows an expanded view close to $T_c$.

of the apparent heat capacity. The latent heat absorbed quasi-isothermally was 33.12 J mol$^{-1}$. These behaviorsare similar to those observed for $x=2.00$. The heat capacity curve is given in Fig. 3.

(iv) $x=1.75$: Figure 4 shows the results of heat capacity measurements on this crystal. The transition temperature was 219.96 K. The first-order component was again observed at the transition temperature. The latent heat of transition is 29.24 J mol$^{-1}$. In the first measurement a small hump was observed around 224 K, some 4 K above the phase transition temperature. In view of the reproducibility of the small peak, presence of impurity in the calorimetric specimen was suspected. Therefore, the heat capacity was measured on a crystal having the same composition but prepared from TCD of a different commercial source. However, in the newly prepared crystal the shoulder appeared at the same temperature. Consequently it was concluded that this phenomenon was intrinsic in the crystal with the composition of $x=1.75$. In the temperature region of this anomally, it took longer time (about 100 min) for the equilibrium with the endothermic temperature drift of 0.3—0.6 mK during the drift period (about 1 h). The phenomenon was reproducible and depended on the pre-cooling condition. It was observed repeatedly when the crystal was cooled below the transition temperature prior to the measurement. When the measurement was started after coolling the sample crystal just 1 K above the transition temperature, the hump in the heat capacity and the associated endothermic effect were not observed.

(v) $x=1.50$: Although latent heat was not observed around the phase transition temperature 221.88 K, the crystal exhibited the highest peak of anomalous heat capacity (500

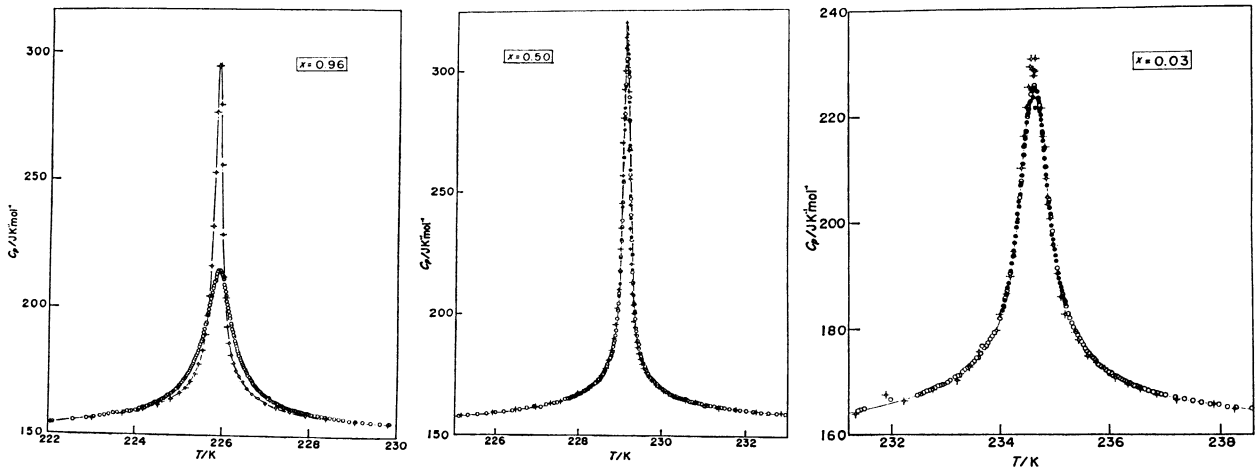


Fig. 7. Aging effect on heat capacity of (a) $x=0.96$, (b) $x=0.50$ and (c) $x=0.03$.
○ and ● : first measurement, -⊙- : measurement for aged crystals.

J $K^{-1}$ $mol^{-1}$) among the crystals having no distinguishable first-order component. However, the equilibration time increased gradually up to 90 min with increase of the heat capacity. Rounding of the heat capacity peak was not observed. At 3 K above the peak temperature, the same phenomena as that found for $x=1.75$ appeared in the temperature drift but the heat capacity hump was not observed. The heat capacity curve is given in Fig. 5.

(vi) $x=0.96$: The anomalous heat capacity due to phase transition is located at 225.92 K and its maximum value is 220 J $K^{-1}$ $mol^{-1}$ which is smaller than those of any other crystal though the annealed crystal shows higher and sharper peak (see below). The peak was rounded within +0.2 K of the transition temperature. The rounding region is slightly wider than those of other crystals. The magnitude and the shape of the heat capacity are similar to those of $x=0.03$.

(vii) $x=0.50$: In this crystal the high resolution measurements were carried out twice before and after the cooling of the crystal down to nitrogen temperature, in order to check the effect of thermal history. Reproducibility of the heat capacity was excellent in all respects including the transition temperature, the maximum value of heat capacity and the rounding region. Rounding phenomenon was found within ±20 mK of the transition temperature (229.15 K) but the maximum of the heat capacity reached 290 J $K^{-1}$ $mol^{-1}$ and is larger than that of $x=0.96$. This corresponds to the narrower region of the peak rounding at this composition of the crystal.

(viii) $x=0.25$: The transition temperature is 230.92 K and the maximum of the peak is 260 J $K^{-1}$ $mol^{-1}$ which is intermediate between those of $x=0.96$ and $x=0.50$ (see Fig. 6). The rounding region is nearly the same as the case of $x=0.50$, and outside of this region the heat capacity due to phase transition is similar to that of $x=0.50$ in respect to the peak width and the sharpness. The measurements of $x=0.03$, $x=0.25$, $x=0.50$, and $x=0.96$ were performed within one month after the preparations of the single crystals. In order to study any effect of aging of the crystals we repeated high resolution measurements for these compositions near the transition temperatures. The sample crystal that had been measured before was used in the renewed measurement for $x=0.50$ and new single crystals of $x=0.03$ and $x=0.96$ were cut from the same ingot from which single crystals used in the earlier measurements were prepared. The time elapsed between the first and the second measurements were four years, ten months, and two years for the $x=0.03$, $x=0.50$,

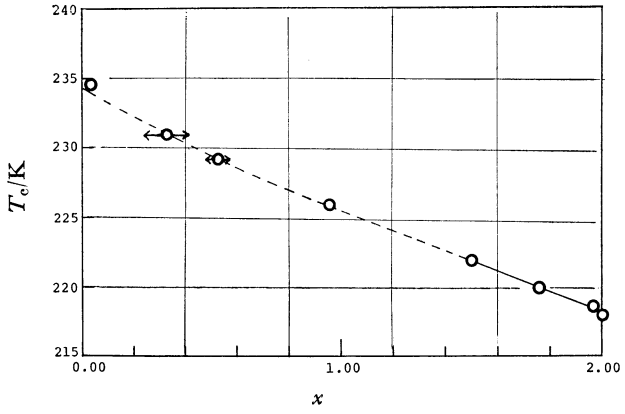


Fig. 8. Transition temperature *vs.* composition of the solid solution. The horizontal arrows indicate the ambiguity of estimation. Meaning of dashed line will be given in the forthcoming paper.

and $x=0.96$, respectively. The crystals had been kept in closed glass jars separately during these periods. For $x=0.96$ and $x=0.50$, the transition temperatures decreased by 30 and 10 mK. In view of the stability of the thermometers discussed earlier,[17] one can attribute the shifts of the transition temperatures to change in the isotopic compositions. The amount of the normal water that had replaced the heavy water during the aging was estimated from the change of the transition temperatures. They are 14 mg in the 47 g crystal of $x=0.96$ and 6 mg in the 60 g crystal of $x=0.50$. It would be reasonable to assume that water of these amount might well had been absorpted on the inner surface of the glass jars when the ingots of the crystal were placed in them and equilibrated with the mixed crystal during the storage. Figure 7 shows the aging effects in anomalous heat capacity of $x=0.96$, $x=0.50$, and $x=0.03$. The anomalous heat capacity in crystal $x=0.96$ increased by a factor of two and became sharper with accompanying the decrease of the rounding region. The peak height of $x=0.50$ increased 3% in the rounding region but the heat capacity was in agreement with the previous results within 0.1% outside the rounding region. In the crystal $x=0.03$ the anomalous heat capacity was reproduced (to 0.1%) in both the temperatures as well as the shape of peak.

*Dependence of Transition Temperature upon the Composition of Solid Solution.* The isotope effect on the transition

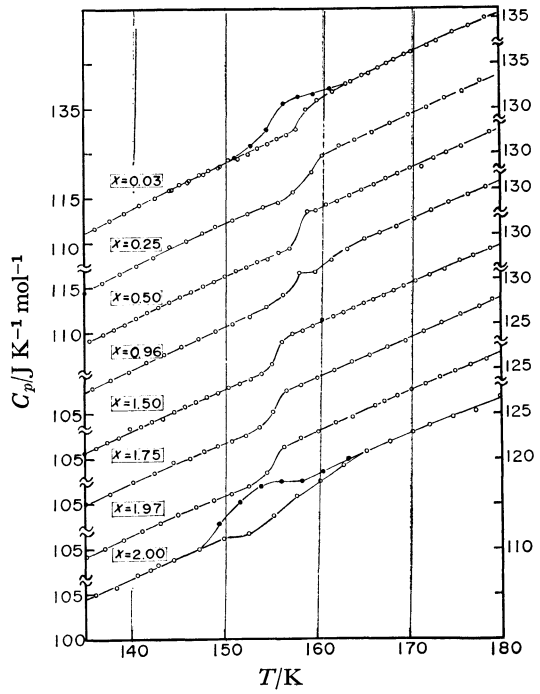


Fig. 9. Heat capacity curves in the region of glass transitions.
Cooling rate; —○— 1.7 K min$^{-1}$, —●— 0.01 K min$^{-1}$.

temperature of the present substance ($T_c^D/T_c^H=1.076$) is of the same order of magnitude as that of a group of hydrogen-bonded ferro- and antiferroelectrics such as $Cu(HCO_2)_2\cdot 4H_2O$,[14] $K_4Fe(CN)_6\cdot 3H_2O$,[19] TGS,[20] TGSe,[21] and Rochelle salt.[22] The relatively small change of $T_c$ on deuteration suggests that the transition is associated with the ordering of the protonic position but is not related to the tunneling motion as in KDP.[23] Figure 8 shows a dependence of transition temperature upon the composition of solid solutions. The observed behavior of $T_c$ against $x$ for the present system is similar to that reported for TGS–DTGS[20] and TGSe–DTGSe[21] systems, where the transition temperature increases monotonously with increasing $x$.

*Glass Transition.* Figure 9 shows the heat capacities in the region of the glass transition for each of the crystals in which those of $x=2.00$ and $x=0.03$ are the results by Matsuo *et al.*[10] The glass transition temperature was found to depend on the isotopic composition (Fig. 10). Here, the glass transition temperature was defined as the temperature where the temperature drift changed from the exothermic to the endothermic.

## Conclusion

We have thus shown that the heat capacities of the mixed crystals $SnCl_2(H_2O)_x(D_2O)_{2-x}$ exhibit two thermal anomalies for the entire range of the isotopic composition. The small isotope effect on the temperature of the relaxational anomaly ($T_g(H_2O)=152.9$ K and $T_g(D_2O)=158.8$ K) may be understood in terms of the smaller vibrational frequency of the deuterium atoms in comparison with the hydrogen. It is important to recognize that glass transition region of the mixed crystals does not split into two. This means that the motions of the hydrogenic atoms are strongly correlated with each other. They migrate in the

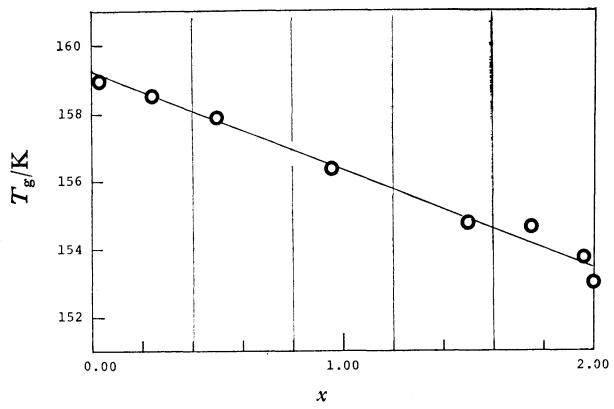


Fig. 10. Concentration dependence of the glass transition temperature.

crystal as a unit whose mobility depends on the local isotopic composition. It appears that the size of the correlation region is large enough that the local composition can be approximated well by the average composition. The smallest unit, and as such the most probable one, is the eight-membered ring of the hydrogen-bonded water molecules, as pointed out previously in relation to the ice condition.[10] The molecular model proposed earlier for the pure $SnCl_2\cdot 2H_2O$ and $SnCl_2\cdot 2D_2O$ thus fits in with the present result on the mixed crystals. Probably the most interesting property of the phase transition in the solid solution is that the first-order component disappears at the composition of 25% deuterium. The disappearance of the first-order nature is not due to inhomogeneity of the isotopic concentration. For, if this were the case, we would have observed the first-order transition also in the $D_2O$-rich crystals because the compositional inhomogeneity is small here again. The experimental fact is that the rounding of the anomalous heat capacity of $x=0.03$ is most extensive. Aging of the crystal for four years did not alter this result. The glass transition at 150 K indicates that the motion of the hydrogen atoms at the transition temperature, $\approx$220 K, is rapid enough that they find the equilibrium distribution during the experimental time scale, provided that possible nonuniformity in the initial isotopic distribution has been homogenized by the aging. The existence of the first-order component in the $H_2O$-righ crystals, its disappearance around $\approx$25% $D_2O$ concentration and the gradual increase of rounding of the anomalous heat capacity in the $D_2O$-rich region are the principal results of the present high resolutional measurements. The correspondence between the liquid-vapor critical point and the phase transition in TCD discussed above has been hinted upon from the structural data. The thermodynamic measurement presented in this study give strong support to the analogy. In the subsequent paper the experimental result will be analysed and discussed in terms of this correspondence.

## References

1) H. Kiriyama and R. Kiriyama, *J. Phys. Soc. Jpn.*, **28**, Suppl., 114 (1970).

2) H. Kiriyama, K. Kitahama, O. Nakamura, and R. Kiriyama, *Bull. Chem. Soc., Jpn.*, **46**, 1389 (1973).
3) R. Kiriyama, H. Kiriyama, K. Kitahama, and O. Nakamura, *Chem. Lett.*, **1973**, 1105.
4) H. Morisaki, H. Kiriyama, and R. Kiriyama, *Chem. Lett.*, **1973**, 1061.
5) C. H. Wang, M. Tatsumi, T. Matsuo, and H. Suga, *J. Chem. Phys.* **67**, 3097 (1977).
6) H. Kiriyama, O. Nakamura, and R. Kiriyama, *Chem. Lett.*, **1976**, 689.
7) K. Kitahama and H. Kiriyama, *Bull. Chem. Soc. Jpn.*, **50**, 3167 (1977).
8) R. Brout, "Phase Transitions," Benjamin Inc., (1965).
9) T. Matsuo, M. Tatsumi, H. Suga, and S. Seki, *Solid State Commun.*, **13**, 1829 (1973).
10) T. Matsuo, M. Oguni, H. Suga, S. Seki, and J. F. Nagle, *Bull. Chem. Soc. Jpn.*, **47**, 57 (1974).
11) S. R. Salinas and J. F. Nagle, *Phys. Rev.*, **B9**, 4920 (1974).
12) P. W. Kasteleyn, *J. Math. Phys.*, **4**, 287 (1963).
13) M. Reiner, *Physics Today*, **17**, 62 (1964).
14) T. Matsuo, M. Kume, H. Suga, and S. Seki, *J. Phys. Chem. Solids*, **37**, 499 (1976).
15) K. Hamano, K. Ema, and Y. Iwana, *J. Phys. Soc. Jpn.*, **44**, 933 (1978).
16) M. Tatsumi, T. Matsuo, H. Suga, and S. Seki, Subsequent paper.
17) M. Tatsumi, T. Matsuo, H. Suga, and S. Seki, *Bull. Chem. Soc. Jpn.*, **48**, 3060 (1975).
18) M. Tatsumi, T. Matsuo, H. Suga, and S. Seki, *J. Phys. Chem. Solids*, **39**, 427 (1978).
19) M. Oguni, T. Matsuo, H. Suga, and S. Seki, *Bull. Chem. Soc. Jpn.*, **48**, 379 (1975).
20) B. Brezina and F. Smutny. *Czech, J. Phys.*, **B18**, 393 (1968).
21) K. Gesi, *J. Phys. Soc. Jpn.*, **41**, 565 (1976).
22) J. Habluetzel, *Helv. Phys. Acta*, **12**, 489 (1939).
23) B. A. Strukov, A. Baddur, V. A. Koptsik, and I. A. Velichko, *Sov. Phys. Solid State*, **14**, 885 (1972).